Journal of Solid State Chemistry **156,** 16–25 (2001)
doi:10.1006/jssc.2000.8951, available online at http://www.idealibrary.com on IDEAL®

Temperature-Dependent Structural Properties and Crystal Twinning in the Fluorocyclohexane/Thiourea Inclusion Compound

Lily Yeo, Kenneth D. M. Harris,[1] and Benson M. Kariuki

School of Chemistry, University of Birmingham, Edgbaston, Birmingham B15 2TT, United Kingdom

Received March 9, 2000; in revised form August 10, 2000; accepted September 5, 2000; published online December 21, 2000

Structural properties of the fluorocyclohexane/thiourea inclusion compound have been investigated as a function of temperature by single-crystal X-ray diffraction. The inclusion compound exhibits different forms of crystal twinning, and we focus on the implementation of methodology for handling twinning in the structure determination process. Differential scanning calorimetry indicates that fluorocyclohexane/thiourea undergoes a solid state phase transition at about 107 K (on cooling). In the high-temperature phase (ambient temperature), fluorocyclohexane/thiourea has the conventional rhombohedral ($R\bar{3}c$) thiourea tunnel structure and the crystal is twinned through coexistence of domains of the obverse and reverse settings of the rhombohedral structure. The guest molecules are substantially disordered, although there is evidence that they are located preferentially in certain regions along the tunnel. In the low-temperature phase, the thiourea tunnel structure is monoclinic ($P2_1/n$), based on a lattice that is close to the orthohexagonal cell of the structure in the high-temperature phase. The host structure is distorted from the rhombohedral tunnel structure of the high-temperature phase, and the guest molecules adopt a preferred orientation with respect to the host structure. The strategy for structure determination of twinned crystals of inclusion compounds applied in this paper should find wider applications to other solid inclusion compounds.

1. INTRODUCTION

Thiourea has been known for some time (1–3) to form crystalline inclusion compounds with a variety of different types of guest molecules. The thiourea tunnel structure has larger cross-sectional area and different symmetry properties from the host tunnel structure in urea inclusion compounds (4, 5), and is consequently able to include bulkier guest molecules containing a wider range of functional group types (4–7). Many research groups have recognized the fact that thiourea inclusion compounds exhibit a diverse range of physico-chemical properties that are of interest from both fundamental and applied perspectives (4, 5).

In general, thiourea inclusion compounds can be classified into two types, characterized by rhombohedral and monoclinic crystal systems. In each case, the host structure is a hydrogen-bonded arrangement of thiourea molecules containing parallel nonintersecting tunnels, within which the guest molecules are located. The tunnel diameter fluctuates significantly on moving along the tunnel (8), giving rise to bulges and constrictions, and in some refflspects it can be more appropriate to regard the thiourea tunnel structure as a "cage"-type host rather than a "tunnel"-type host. In general, the rhombohedral host structure is formed for guest molecules that are substantially isotropic in shape, and there is usually considerable dynamic disorder of the guest molecules. In many cases, this rhombohedral structure undergoes a low-temperature phase transition to a structure of lower symmetry (usually monoclinic), representing a deformation of the tunnel and an increase in the orientational ordering of the guest molecules. On the other hand, for guest molecules that are more planar in shape, the host structure at ambient temperature tends to be a distorted form of the rhombohedral structure, and the guest molecules often adopt an ordered arrangement.

Thiourea inclusion compounds containing monosubstituted and disubstituted cyclohexane guest molecules have been the subject of a number of studies, particularly concerning the conformational properties of the guest molecules and comparisons with the conformational properties of the same molecules in other phases (9–15). Interestingly, the conformational properties of fluorocyclohexane ($C_6H_{11}F$) guest molecules in the thiourea tunnel structure (16, 17) differ significantly from those of other monohalogenocyclohexane guest molecules ($C_6H_{11}X$, for X = Cl, Br, and I). For fluorocyclohexane, there are approximately equal amounts of guest molecules in the axial and equatorial conformations (16, 17), whereas the other monohalogenocyclohexane guest molecules have a substantial excess of the axial conformation (12) (mole fraction in the range 0.85 to

[1] To whom correspondence should be addressed.

0022-4596/01 $35.00

0.95 at ambient temperature) inside the thiourea tunnel structure.

Here we report variable-temperature single-crystal X-ray diffraction studies of the thiourea inclusion compound containing fluorocyclohexane guest molecules. These studies are also of fundamental interest as the structure determination is complicated by the existence of different forms of crystal twinning in this inclusion compound.

2. CRYSTAL TWINNING

Twinned crystals comprise two or more individual fragments that have the same crystal structure but different orientations. Several different schemes for classification of twinned structures have been developed (18–24). As discussed below, the fluorocyclohexane/thiourea inclusion compound has the conventional rhombohedral thiourea tunnel structure (space group $R\bar{3}c$) in the high-temperature phase, and contains separate domains (twin components) representing the obverse and reverse settings of the rhombohedral structure. In this example, twinning is introduced during the crystal growth process. In the low-temperature phase, the structure becomes monoclinic (space group $P2_1/n$) and the crystals remain twinned.

The obverse and reverse settings of a rhombohedral system are related by 180° (or 60° or 300°) rotation of the structure about the **c** axis of the hexagonal cell. The orientation of the hexagonal cell is identical for the obverse and reverse twin components, but the two lattice points inside the hexagonal cell (arising from the rhombohedral centering) are in different positions for the obverse and reverse settings. The lattice centering in the obverse setting gives the condition $-h+k+l=3n$ (n = integer) for the presence of reflections, whereas the lattice centering in the reverse setting gives the condition $h-k+l=3n$ (n = integer). For a crystal containing twin domains of both the obverse and reverse settings, each observed reflection with $l \neq 3n$ arises from scattering by either the obverse domain or the reverse domain, but not both. However, each observed reflection with $l=3n$ has a contribution from the obverse domain *and* a contribution from the reverse domain. The orientational relationship between the obverse and reverse domains is shown in Fig. 1, and the reorientation required to transform from the obverse setting to the reverse setting is defined by the transformation

$$(a,\ b,\ c)_{\text{reverse}} = (a,\ b,\ c)_{\text{obverse}} \begin{pmatrix} -1 & 0 & 0 \\ 0 & -1 & 0 \\ 0 & 0 & 1 \end{pmatrix}.$$

The same matrix is required to transform the diffraction data (h, k, l):

$$(h,\ k,\ l)_{\text{reverse}} = (h,\ k,\ l)_{\text{obverse}} \begin{pmatrix} -1 & 0 & 0 \\ 0 & -1 & 0 \\ 0 & 0 & 1 \end{pmatrix}.$$

For convenience, we use the notation [− 1 0 0/0 − 1 0/0 0 1] to represent the above 3×3 matrix. On the assumption of Friedel's Law, an equivalent transformation of the diffraction data from the obverse setting to the reverse setting is defined by the matrix [1 0 0/0 1 0/0 0 − 1].

3. EXPERIMENTAL

The fluorocyclohexane/thiourea inclusion compound was prepared from commercially available reagents as follows.

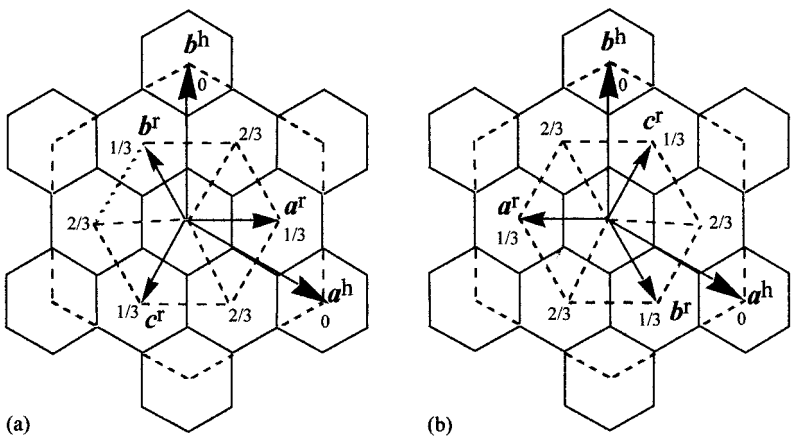

FIG. 1. Definition of (a) the obverse setting and (b) the reverse setting of the rhombohedral description $\{\mathbf{a}^r, \mathbf{b}^r, \mathbf{c}^r\}$ of the structure of thiourea inclusion compounds at ambient temperature, and their relationship to the hexagonal description $\{\mathbf{a}^h, \mathbf{b}^h, \mathbf{c}^h\}$. The lattice vectors $\mathbf{a}^h$ and $\mathbf{b}^h$ lie parallel to the plane of the page and $\mathbf{c}^h$ is perpendicular to the page, whereas $\mathbf{a}^r$, $\mathbf{b}^r$, and $\mathbf{c}^r$ are directed outward from the plane of the page. The projections of the thiourea tunnels are shown. Numbers given at the termini of vectors indicate height (perpendicular to the page) as a multiple of $\mathbf{c}^h$.

Fluorocyclohexane was added to a saturated solution of thiourea in methanol in a conical flask under ultrasonic agitation at 328 K (the fluorocyclohexane:thiourea molar ratio in solution was taken in excess of the normal 1:3 stoichiometry of thiourea inclusion compounds). The flask was then transferred to an incubator and cooled systematically from 328 to 288 K over a period of 24 hours. When sufficiently large crystals had grown (after a few days), they were collected and washed with 2,2,4-trimethylpentane. The crystals were dried briefly on filter paper and stored in a sealed container at 4°C (note that fluorocyclohexane/thiourea tends to decompose slowly when left in an open atmosphere at ambient temperature). From optical microscopy, the crystals have long hexagonal needle morphology and are uniaxial (the needle axis is the optic axis). Powder X-ray diffraction confirmed that the samples have the conventional rhombohedral thiourea host structure at ambient temperature. In general, a small amount of the pure crystalline phase of thiourea is also present.

Differential scanning calorimetry was carried out using a Perkin–Elmer DSC-7 instrument, with the polycrystalline sample of fluorocyclohexane/thiourea subjected to cooling and heating cycles at a rate of $10\ \mathrm{K\ min^{-1}}$. The results provide clear evidence for a phase transition at 106.6 K (exotherm) in the cooling cycle and at 107.6 K (endotherm) in the subsequent heating cycle (the quoted temperatures are onset temperatures). We refer to temperatures above and below this transition as the high-temperature and low-temperature phases respectively.

Single-crystal X-ray diffraction studies of fluorocyclohexane/thiourea were carried out using graphite-monochromated Mo$K\alpha$ radiation ($\lambda = 0.71073$ Å) on a Rigaku R-Axis II single-crystal X-ray diffractometer equipped with an image plate detector. Following data collection at ambient temperature, a different crystal was used for the experiments at low temperature, as the crystals were found to decompose slowly under X-ray irradiation. A standard MSC low-temperature device employing a liquid nitrogen cryostat was used for these experiments. At the low end of the accessible temperature range, the accuracy of this device is estimated to be in the region of ± 5 K. As it was not certain whether the low-temperature phase could actually be reached using this low-temperature device (for which the lowest nominal temperature in our previous experience was approx. 105 K), a series of single crystal X-ray diffraction rotation photographs were recorded for fluorocyclohexane/thiourea in the region of the lowest attainable temperatures. At the lowest temperature (nominally measured as 111 K from the thermocouple in the cryostat), a significant change in the rotation photograph was observed (see discussion in Section 4.2), implying that a transition to the low-temperature phase had taken place. The crystal was kept for 2 h at this temperature, to ensure that thermal equilibrium was reached, before starting the X-ray diffraction data collection. Although the nominal temperature (111 K) of this data collection is higher than the phase transition temperature (107 K) determined from the cooling cycle in our DSC experiments, the structural information determined from these data is clearly consistent with a low-temperature phase. Furthermore, data analysis did not encounter any difficulties of the type that would arise if the temperature during the data collection had been fluctuating across the phase transition temperature. The discrepancy between the nominal temperature (111 K) of the data collection and the presumed actual temperature (less than 107 K) of the data collection presumably reflects systematic errors in the temperature measurements. In this regard, the determination of the phase transition temperature from our differential scanning calorimetry experiments is considered to be substantially more accurate than the temperature measurements of the single-crystal X-ray diffraction data collection.

TABLE 1
Data Collection Parameters for the Single-Crystal X-Ray Diffraction Experiments

Inclusion compound	$C_6H_{11}F$/thiourea	
Temperature (K)	293	111
No. of frames recorded	36	90
Oscillation angle per frame (°)	5	2
Exposure time per frame (min)	25	15
Crystal-to-detector distance (mm)	80	100

Note. $C_6H_{11}F$ represents fluorocyclohexane.

Parameters relating to single crystal X-ray diffraction data collection are summarized in Table 1. Data reduction was carried out using standard methods in the TEXSAN software (25) and no absorption correction was applied. Structure solution was carried out using the direct methods program SIR-92 (26) and structure refinement was carried out using the program SHELXL-97 (27). Standard agreement factors R and R_w were considered.

To provide a qualitative understanding of the diffraction patterns, single-crystal X-ray diffraction rotation photographs were recorded at the same temperatures as the data collections, with the rotation axis parallel to the needle axis of the crystal morphology (tunnel axis of the thiourea host structure).

4. RESULTS AND DISCUSSION

4.1. High-Temperature Phase

Powder X-ray diffraction at ambient temperature indicates that the fluorocyclohexane/thiourea inclusion compound has the conventional rhombohedral thiourea host structure. The single-crystal X-ray diffraction rotation photograph is shown in Fig. 2. The positions of all reflections in

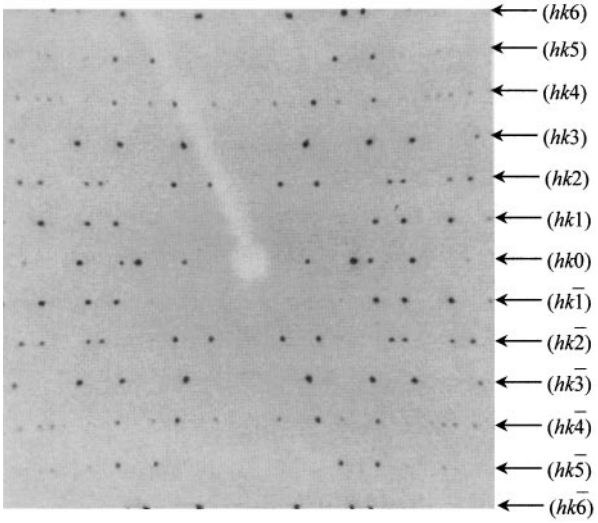

FIG. 2. Single-crystal X-ray diffraction rotation photograph recorded at 293 K for the fluorocyclohexane/thiourea inclusion compound rotating about the tunnel axis. Layer lines (horizontal) of the diffraction pattern are indexed.

the X-ray diffraction pattern can be rationalized on the basis of a single reciprocal lattice with three-dimensional periodicity, implying that the inclusion compound is commensurate (see Refs. (28) and (29) for a discussion of the distinction between commensurate and incommensurate inclusion compounds). The lattice has hexagonal metric symmetry: $a = b = 15.97$ Å, $c = 12.50$ Å, $\alpha = \beta = 90°$, $\gamma = 120°$. The Laue group is $\bar{3}m$, with the following conditions for the presence of reflections: [A] (h, k, i, l), $-h + k + l = 3n$ or $h - k + l = 3n$ (with the following consequences of these conditions, (h, h, $\bar{2h}$, l), $l = 3n$; (h, 0, $\bar{h}$, l): $h + l = 3n$ or $-h + l = 3n$); [B] (h, 0, $\bar{h}$, l): $l = 2n$; [C] (0, 0, 0, l), $l = 6n$. The conditions given under [A] indicate that there is lattice centering characteristic of a rhombohedral system with *both* the obverse and reverse settings present. Condition [B] is characteristic of a c-glide plane and condition [C] arises from the combination of [A] and [B]. As discussed in Section 2, each observed reflection with $l \neq 3n$ arises from scattering by one or other of the twin domains (but not both), whereas each observed reflection with $l = 3n$ is a superposition of a reflection from each twin domain. The orientational relationships between the rhombohedral lattices of the obverse and reverse settings and the corresponding hexagonal lattice are shown in Fig. 1.

The systematic absences are consistent with space group $R\bar{3}c$, as found for other thiourea inclusion compounds. Comparison of the intensities of corresponding reflections (with $l \neq 3n$) that arise uniquely from the obverse domain and the reverse domain suggests that the volume fractions of the two twin domains in the crystal studied are approximately 85% (obverse) and 15% (reverse). As the proportion of the reverse domain is rather small, structure solution was initially attempted using those reflections with $l \neq 3n$ that arise uniquely from the obverse domain plus all reflections with $l = 3n$. We note that each reflection with $l = 3n$ contains some "contamination" from the reverse domain, but as the volume fraction of the reverse domain is small, this contamination may not cause serious problems in structure solution. Full consideration of both twin components was introduced at the structure refinement stage (see below). Structure solution allowed the nonhydrogen atoms of the thiourea host structure to be located. This "host-only" structure was then used as the initial structural model for structure refinement.

In refinement of twinned structures using the SHELXL-97 program (27), the structure factor amplitude F_c^2 is calculated by

$$F_c^2 = S^2 \sum_{m=1}^{n} k_m (F_{c,m})^2,$$

where S is the overall scale factor, n is the number of twin domains, k_m is the fractional contribution of twin domain m, and $(F_{c,m})^2$ is the calculated structure factor amplitude for twin domain m. As we require that

$$\sum_{m=1}^{n} k_m = 1,$$

only $n - 1$ of the fractional occupancies (k_2, k_3, …, k_n) require to be refined (30).

As some reflections contain contributions from both twin domains whereas other reflections arise only from one twin domain, the input to the SHELXL-97 structure refinement program requires each reflection to be labeled with a twin identification number specifying the twin domain (obverse and/or reverse) that contributes to its intensity. Also, we require to transform the Miller indices for the reverse twin to the corresponding Miller indices in the obverse setting. Thus, the input data for structure refinement were prepared as follows. First, reflections were merged assuming space group $P321$ (to ensure that no reflections were rejected on the basis of rhombohedral lattice centering) and Laue group $\bar{3}m$. Next, for reflections with $l \neq 3n$ (each of which contains a contribution from only one twin domain), the reflections with $-h + k + l = 3n$ (obverse twin) were assigned as twin number 1 and the reflections with $h - k + l = 3n$ (reverse twin) were assigned (following transformation into the indices of the obverse setting) as twin number 2. For reflections with $l = 3n$ (each of which contains a contribution from both twin domains), two sets of reflections were generated. For the first set, the (h, k, l) indices were taken to be the same as the measured diffraction data and assigned as twin number 1. For the second set, the (h, k, l) indices were transformed to (h, k, $\bar{l}$) (see Section 2) and assigned as twin

number − 2. The fractional contributions of the two twin domains were initially taken to be equal and the fraction k_2 was refined (note that $k_1 = 1 - k_2$).

In common with other thiourea inclusion compounds, the guest molecules in fluorocyclohexane/thiourea are likely to exhibit some degree of positional ordering (although not necessarily orientational ordering) with respect to the host structure (31), and the method for handling the guest substructure in the structure determination calculations requires particular attention. For the nonhydrogen atoms of thiourea, atomic coordinates (taken initially from the structure solution) and displacement parameters (ultimately anisotropic) were refined in the conventional manner. The difference Fourier map for this "host-only" structure contains significant maxima within the tunnel, representing electron density from the disordered guest molecules. A carbon atom was added in the position of the highest maximum in the difference Fourier map, and its positional parameters and isotropic displacement parameter were refined together with the parameters for the nonhydrogen atoms of the host structure. This procedure was repeated, adding one carbon atom at a time, until the highest peak in the difference Fourier map represented the position of a thiourea hydrogen atom. As expected, the refined isotropic displacement parameters for the carbon atoms in the tunnel were significantly higher than the equivalent isotropic displacement parameters for the thiourea atoms. Finally, hydrogen atoms were added to the thiourea molecules according to standard geometries and were refined using a "riding" model in which the same coordinate shifts were applied to a given hydrogen atom and the nitrogen atom to which it is bonded. The isotropic displacement parameter of each hydrogen atom was taken as 1.2 times the equivalent isotropic displacement parameter of the nitrogen atom to which it is bonded.

The final refined structure is viewed along the tunnel axis in Fig. 3 and structural parameters are given in Table 2. The refined fractional occupancies of the two twin components were 0.85(1) (obverse domain) and 0.15(1) (reverse domain), in close agreement with the fractional contributions estimated above.

Although the refined positions of the atoms inside the host tunnel do not represent a meaningful structure for an individual fluorocyclohexane molecule, the guest electron density is nevertheless localized in certain regions along the tunnel, corresponding to preferred locations of the orientationally disordered guest molecules. The refined isotropic displacement parameters for these guest atoms are large, clearly representing a smeared out (although nonuniform) time-averaged electron density distribution within the tunnel. Such structural disorder of the guest molecules is consistent with conclusions from solid state NMR studies (14,16,17).

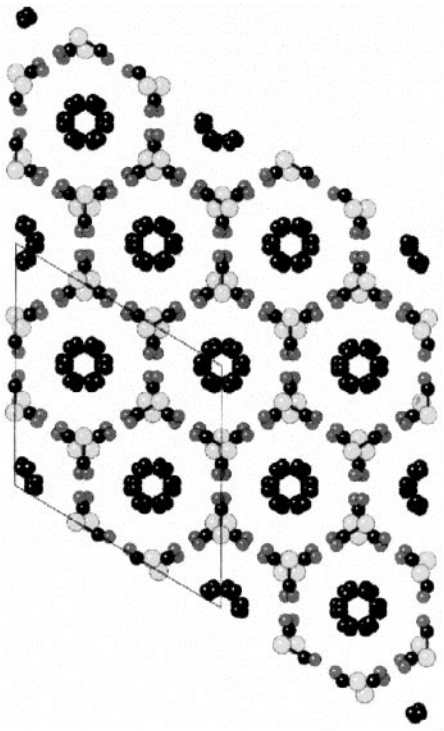

FIG. 3. Structure of the fluorocyclohexane/thiourea inclusion compound determined at 293 K, viewed along the **c** axis (tunnel direction). The atoms within the tunnel have been added to represent the contribution to the diffraction pattern from scattering by the guest molecules. The extent to which physical interpretation can be given to the refined positions of these atoms is discussed in the text. Color code: sulfur, light gray; carbon, black; nitrogen, medium gray.

4.2. Low-Temperature Phase

Figure 4 shows the single-crystal X-ray diffraction rotation photograph recorded for fluorocyclohexane/thiourea in the low-temperature phase (see Section 3). There is no evidence for the evolution of any superstructure along the tunnel direction in the low-temperature phase, but the number and arrangement of diffraction maxima within the layer lines are different in the low-temperature and high-temperature phases. The metric symmetry in the low-temperature phase is orthorhombic, and the lattice ($a = 27.52$ Å, $b = 15.72$ Å, $c = 12.33$ Å, $\alpha = \beta = \gamma = 90^\circ$) is apparently based on the orthohexagonal description of the rhombohedral structure of the high-temperature phase. However, the Laue symmetry is actually monoclinic $2/m$ and systematic absences are consistent with space group $P2_1/n$. The orientational relationship between the rhombohedral lattice and the orthohexagonal description is shown in Fig. 5.

On passing into the low-temperature phase, the Laue symmetry is lowered from $\bar{3}m$ to $2/m$. For the high-temperature phase, the rhombohedral lattice centering means that each observed reflection with $l \neq 3n$ arises either from one domain or the other domain, and cannot have contributions

TABLE 2
Structural Parameters Determined for the Fluorocyclohexane/Thiourea Inclusion Compound at 293 K, and Other Information Relating to the Structure Refinement Calculations

Space group	$R\bar{3}c$
Lattice parameters	$a = 15.971(3)$ Å
	$c = 12.495(2)$ Å
No. of unique reflexions with $\|F_o\| > 4\sigma(F_o)$	881
R	0.1489
R_w	0.4134
Weight	$1/[\sigma(F_o)^2 + (0.1623*P)^2 + 28.99*P]$ where $P = [\max(F_o^2, 0) + 2F_c^2]/3$
No. of parameters refined	29

Atom	x/a	y/b	z/c	U_{11}(Å^2)	U_{22}(Å^2)	U_{33}(Å^2)	U_{23}(Å^2)	U_{13}(Å^2)	U_{12}(Å^2)
S1	0.6999(2)	0.0000(0)	0.2500(0)	0.065(2)	0.084(3)	0.057(2)	− 0.005(1)	− 0.0025(7)	0.042(1)
N1	0.5417(6)	− 0.0178(7)	0.1607(7)	0.076(6)	0.123(8)	0.067(5)	− 0.004(5)	− 0.012(4)	0.060(6)
C1	0.5929(10)	0.0000(0)	0.2500(0)	0.080(7)	0.076(9)	0.068(8)	0.011(7)	0.006(3)	0.038(5)

Atom	x/a	y/b	z/c	U_{iso} (Å^2)	Bond Length (Å)		Bond Angle (°)	
C2	0.612(6)	0.250(4)	0.192(5)	0.42(3)	C1–S1	1.71(2)	S1–C1–N1	120.6(7)
C3	0.561(3)	0.296(5)	0.134(4)	0.36(2)	C1–N1	1.33(1)		

Note. C2 and C3 denote carbon atoms added within the tunnel to represent the contribution to the diffraction pattern from scattering by the guest molecules. The asymmetric unit of the host substructure comprises one-half thiourea molecule, with its S=C bond lying along a crystallographic two-fold symmetry axis (special position $(x, 0, \frac{1}{4})$), whereas N occupies a general position. There are six thiourea molecules in the unit cell.

from both domains. However, for the low-temperature phase, the rhombohedral lattice centering is lost and there is no restriction that reflections with $l \neq 3n$ must only have a contribution from one domain. Thus, every observed reflection may contain a contribution from both twin domains (such twinning is described as merohedral).

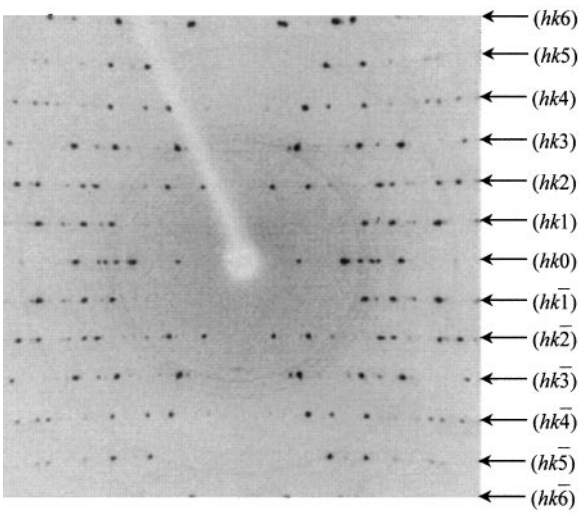

FIG. 4. Single-crystal X-ray diffraction rotation photograph recorded in the low-temperature phase (see Section 3) for the fluorocyclohexane/thiourea inclusion compound rotating about the tunnel axis. Layer lines (horizontal) of the diffraction pattern are indexed.

On this basis, our structure solution calculation (using direct methods) for space group $P2_1/n$ used all the measured diffraction data. All nonhydrogen atoms of the thiourea host structure were located and this "host-only" structure was then used as the initial model for structure refinement. To take merohedral twinning into account in the structure refinement requires knowledge of the twin law that relates the two twin components. In this case, the twin law originates from the obverse/reverse twinning in the high-temperature phase and may be described by the matrix [1 0 0/ 0 − 1 0/0 0 − 1] (representing 180° rotation about the a° axis—see Fig. 5). The fractional contributions of the two twin domains were initially taken to be equal and the fraction k_2 was refined.

The difference Fourier map for the refined "host-only" structural model contained significant peaks inside the tunnel. To introduce this guest electron density into the model, the strategy described in Section 4.1 was followed. However, as refinement of twinned crystals with large asymmetric units can suffer from problems of stability (there are nine thiourea molecules in the asymmetric unit in the present case), it was found necessary to introduce additional restraints in the refinement. Thus, the C–S and C–N bond lengths of the thiourea molecules were restrained to a common value for each type of bond (effective standard deviation 0.02) and "rigid bond" restraints were used (i.e., the components of anisotropic displacement in the direction of the bond were restrained to be equal for the two atoms forming the bond, with effective standard deviation 0.01).

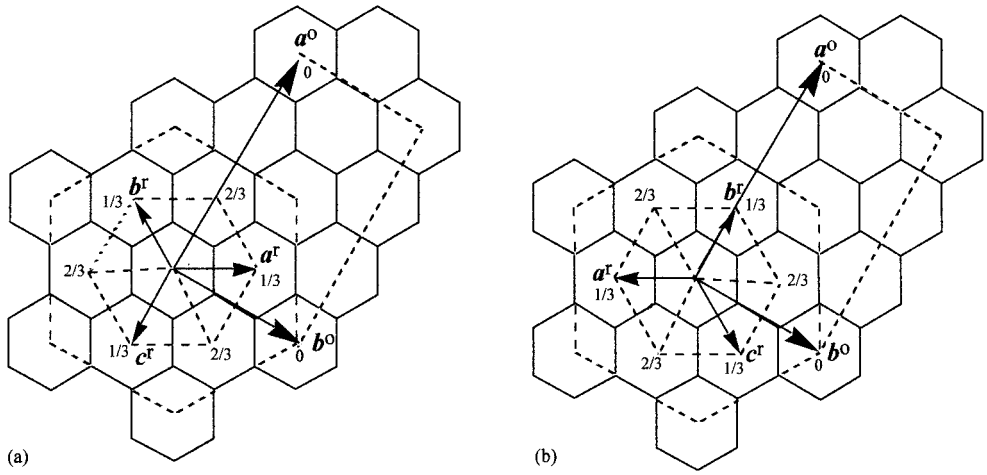

FIG. 5. The obverse (a) and reverse (b) settings of the rhombohedral lattice $\{\mathbf{a}^r, \mathbf{b}^r, \mathbf{c}^r\}$ and their relationship to the orthohexagonal description $\{\mathbf{a}^o, \mathbf{b}^o, \mathbf{c}^o\}$. The structure of the fluorocyclohexane/thiourea inclusion compound is based on the rhombohedral lattice in the high-temperature phase and based on the orthorhombic lattice in the low-temperature phase (although the Laue symmetry is actually monoclinic, as discussed in the text). The lattice vectors $\mathbf{a}^o$ and $\mathbf{b}^o$ are parallel to the plane of the page and $\mathbf{c}^o$ is perpendicular to the page, whereas $\mathbf{a}^r$, $\mathbf{b}^r$ and $\mathbf{c}^r$ are directed outward from the plane of the page. Numbers given at the termini of vectors indicate height (perpendicular to the page) as a multiple of $\mathbf{c}^o$.

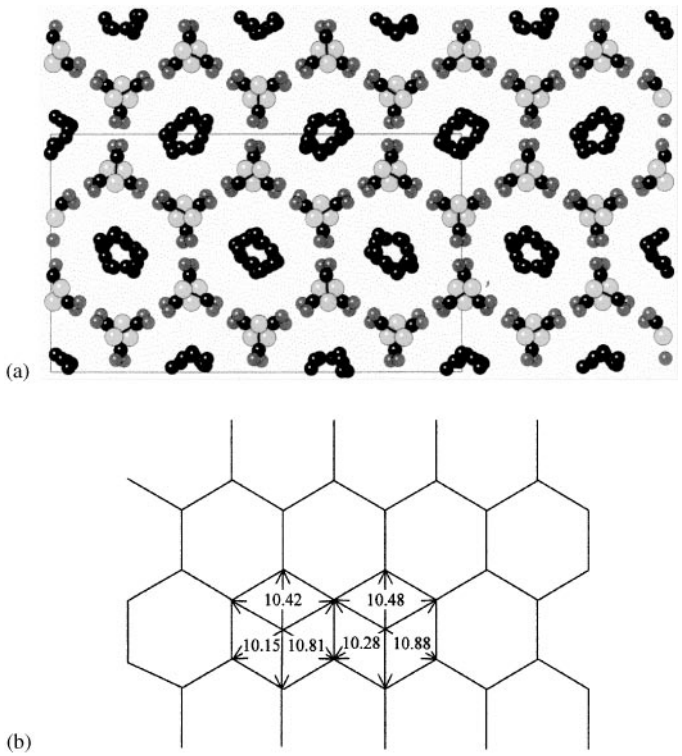

FIG. 6. (a) Structure of the fluorocyclohexane/thiourea inclusion compound in the low-temperature phase (see Section 3), viewed along the **c** axis (tunnel direction). The atoms within the tunnel have been added to represent the contribution to the diffraction pattern from scattering by the guest molecules. The extent to which physical interpretation can be given to the refined positions of these atoms is discussed in the text. Color code: sulfur, light gray; carbon, black; nitrogen, medium gray. (b) Schematic diagram of the host structure in the low-temperature phase (see Section 3), illustrating the distortion of the projection of the thiourea host tunnels from hexagonal geometry (distances are given in Å units).

Structure refinement proceeded satisfactorily and the fractional occupancies of the twin components converged to 0.69(1) and 0.31(1). The fact that these fractional occupancies differ from those determined at ambient temperature reflects the use of different crystals at each temperature, rather than signifying any intrinsic temperature dependence of the twinning.

The final refined structure in the low-temperature phase is viewed along the tunnel axis in Fig. 6 and structural parameters are given in Table 3. The host structure represents a distorted form of the host structure of the high-temperature phase, and contains two crystallographically independent types of tunnel. Although the Laue symmetry is strictly monoclinic, the lattice is based approximately on the orthohexagonal description of the metric symmetry of the high-temperature phase. The projections of the tunnels onto the plane perpendicular to the tunnel axis are distorted hexagons, with one "diameter" between opposite corners of the hexagon longer than the other two "diameters" (Fig. 6). The guest molecules remain substantially disordered in the low-temperature phase (in contrast to the situation for chlorocyclohexane/thiourea in its low-temperature phase (32), for which well-defined positions for the atoms of the guest molecules are identified). Solid state ^{13}C and ^{19}F NMR (14, 16, 17) studies of fluorocyclohexane/thiourea have shown that both the axial and equatorial conformations of the guest molecules are present in essentially equal proportions (interconverting through ring inversion), whereas for other monohalogenocyclohexane guest molecules ($C_6H_{11}X$, for $X = Cl$, Br, I) the axial conformation predominates (9–15). The greater conformational disorder for fluorocyclohexane may underlie the fact that well-defined atomic positions for the guest molecules cannot be

TABLE 3
Structural Parameters Determined for the Fluorocyclohexane/Thiourea Inclusion Compound at 111 K, and Other Information Relating to the Structure Refinement Calculations

Space group	$P2_1/n$
Lattice parameters	$a = 27.52(2)$ Å $b = 15.718(8)$ Å $c = 12.33(2)$ Å $\beta = 90^\circ$
No. of unique reflexions with $\|F_o\| > 4\sigma(F_o)$	4523
R	0.1481
R_w	0.3989
Weight	$1/[\sigma(F_o)^2 + (0.1000*P)^2]$, where $P = [\max(F_o^2, 0) + 2F_c^2]/3$
No. of parameters refined	438

Atom	x/a	y/b	z/c	U_{11}(Å^2)	U_{22}(Å^2)	U_{33}(Å^2)	U_{23}(Å^2)	U_{13}(Å^2)	U_{12}(Å^2)
C1	0.5280(3)	− 0.2080(5)	0.5861(6)	0.052(6)	0.023(5)	0.032(5)	− 0.006(4)	− 0.011(4)	− 0.000(4)
N1	0.5448(3)	− 0.2419(5)	0.4956(5)	0.031(4)	0.042(5)	0.048(4)	− 0.005(3)	− 0.006(3)	0.013(4)
N2	0.5557(3)	− 0.2109(6)	0.6749(6)	0.059(6)	0.084(7)	0.034(4)	0.000(4)	− 0.023(4)	− 0.010(5)
S1	0.4749(1)	− 0.1466(2)	0.5848(2)	0.047(2)	0.0533(2)	0.035(2)	− 0.005(1)	0.007(1)	0.010(1)
C2	0.4580(3)	− 0.2059(6)	− 0.0828(5)	0.050(6)	0.052(6)	0.008(4)	0.000(3)	− 0.002(3)	− 0.003(5)
N3	0.4305(3)	− 0.2055(5)	− 0.1706(5)	0.040(5)	0.076(6)	0.030(4)	0.007(4)	− 0.008(4)	0.010(4)
N4	0.4392(3)	− 0.2353(5)	0.0078(5)	0.046(5)	0.079(7)	0.028(4)	0.014(4)	− 0.008(3)	− 0.019(4)
S2	0.5117(1)	− 0.1489(2)	− 0.0803(2)	0.059(2)	0.049(2)	0.032(1)	0.001(1)	− 0.008(1)	− 0.014(1)
C3	0.3297(3)	− 0.4066(5)	0.0837(6)	0.040(6)	0.027(5)	0.038(5)	− 0.023(3)	− 0.006(4)	− 0.016(4)
N5	0.3215(3)	− 0.4508(6)	0.1728(5)	0.067(6)	0.087(6)	0.025(4)	− 0.003(4)	0.002(4)	− 0.018(5)
N6	0.3412(3)	− 0.4472(5)	− 0.0062(5)	0.078(7)	0.041(5)	0.034(5)	0.003(3)	0.009(4)	0.008(5)
S3	0.3251(1)	− 0.2953(2)	0.0845(2)	0.067(2)	0.048(2)	0.031(2)	− 0.009(1)	0.009(1)	0.005(1)
C4	0.6202(3)	− 0.3037(6)	0.0874(6)	0.052(6)	0.039(6)	0.038(5)	0.006(4)	− 0.003(4)	− 0.003(5)
N7	0.6065(3)	− 0.2619(5)	0.1724(5)	0.058(6)	0.072(6)	0.027(4)	0.006(4)	− 0.008(3)	0.019(5)
N8	0.5970(3)	− 0.2915(6)	− 0.0034(6)	0.069(6)	0.083(7)	0.027(4)	− 0.001(4)	− 0.001(4)	0.025(5)
S4	0.6779(1)	− 0.3481(2)	0.0841(2)	0.041(2)	0.044(2)	0.038(1)	− 0.009(1)	0.001(1)	− 0.017(1)
C5	0.3625(3)	− 0.2976(6)	0.4163(6)	0.056(6)	0.063(7)	0.024(5)	− 0.007(4)	0.013(4)	− 0.008(5)
N9	0.3775(3)	− 0.2588(5)	0.3279(5)	0.063(6)	0.061(6)	0.025(4)	− 0.011(3)	0.016(4)	0.001(4)
N10	0.3880(3)	− 0.2874(5)	0.5051(5)	0.043(5)	0.078(6)	0.036(4)	0.001(4)	0.012(3)	− 0.045(5)
S5	0.3086(1)	− 0.3523(2)	0.4194(2)	0.045(2)	0.057(2)	0.037(2)	− 0.003(1)	− 0.014(1)	− 0.002(1)
C6	0.6624(4)	− 0.4059(5)	0.4148(5)	0.053(7)	0.057(6)	0.023(5)	− 0.008(4)	0.012(4)	0.021(5)
N11	0.6731(3)	− 0.4516(5)	0.3287(5)	0.066(6)	0.071(6)	0.021(4)	− 0.013(3)	0.016(4)	0.016(5)
N12	0.6553(4)	− 0.4492(5)	0.5078(5)	0.110(8)	0.034(5)	0.020(4)	− 0.016(3)	− 0.001(4)	0.011(5)
S6	0.6577(1)	− 0.2959(2)	0.4183(2)	0.066(2)	0.045(2)	0.036(2)	0.001(1)	0.004(1)	0.006(1)
C7	0.4942(4)	− 0.0937(5)	0.2522(6)	0.0726(7)	0.036(5)	0.037(5)	− 0.030(4)	− 0.007(5)	0.020(5)
N13	0.50630(4)	− 0.0547(5)	0.16230(6)	0.095(8)	0.047(5)	0.048(4)	− 0.003(4)	− 0.019(5)	0.007(5)
N14	0.4877(3)	− 0.0495(5)	0.3416(6)	0.062(6)	0.036(5)	0.053(5)	− 0.026(4)	0.008(4)	− 0.001(4)
S7	0.49343(8)	− 0.2033(2)	0.2512(1)	0.030(1)	0.042(2)	0.031(1)	− 0.0111(9)	0.007(1)	0.007(1)
C8	0.1953(3)	0.7951(6)	0.2496(6)	0.030(5)	0.062(7)	0.046(5)	− 0.019(5)	0.007(5)	0.007(5)
N15	0.2133(4)	0.7582(6)	0.1651(5)	0.081(7)	0.086(7)	0.028(4)	− 0.001(4)	0.004(4)	0.039(6)
N16	0.2214(3)	0.7880(5)	0.3398(5)	0.057(5)	0.045(5)	0.030(4)	0.003(3)	0.011(3)	0.006(4)
S8	0.1417(1)	0.8537(2)	0.2510(2)	0.047(1)	0.040(2)	0.031(1)	− 0.002(1)	0.011(1)	0.0033(7)
C9	0.7901(3)	− 0.2039(6)	0.2512(6)	0.037(5)	0.039(6)	0.039(5)	0.007(4)	0.004(4)	0.001(4)
N17	0.7637(3)	− 0.2094(5)	0.1616(5)	0.031(4)	0.071(6)	0.038(4)	0.006(4)	0.000(3)	− 0.014(4)
N18	0.7742(3)	− 0.2377(4)	0.3406(5)	0.071(6)	0.038(5)	0.036(4)	− 0.003(3)	0.008(4)	− 0.012(4)
S9	0.8454(1)	− 0.1494(2)	0.2504(2)	0.049(2)	0.074(2)	0.034(2)	0.000(1)	0.003(1)	− 0.018(1)

Atom	x/a	y/b	z/c	U_{iso} (Å^2)	Atom	x/a	y/b	z/c	U_{iso} (Å^2)
C10	0.051(1)	0.035(2)	0.191(2)	0.166(8)	C11	0.157(3)	0.585(4)	1.060(4)	0.50(4)
C12	0.124(1)	0.528(2)	0.468(2)	0.175(9)	C13	0.2010(7)	0.458(1)	0.358(1)	0.120(6)
C14	0.153(1)	0.441(2)	0.522(2)	0.175(9)	C15	− 0.027(1)	− 0.056(2)	0.192(3)	0.23(1)
C16	0.136(1)	0.548(2)	0.343(2)	0.166(9)	C17	0.0177(9)	− 0.045(2)	0.146(2)	0.154(8)
C18	− 0.043(1)	− 0.018(2)	0.326(2)	0.20(1)	C19	0.221(2)	0.496(3)	0.853(4)	0.30(2)
C20	0.184(2)	0.442(3)	0.855(4)	0.34(2)	C21	0.1852(9)	0.540(2)	0.309(2)	0.161(8)
C22	0.142(2)	0.447(3)	1.330(4)	0.38(3)	C23	0.146(1)	0.447(2)	1.028(3)	0.22(1)

TABLE 3—*Continued*

Atom	x/a	y/b	z/c	U_{iso} (Å^2)	Atom	x/a	y/b	z/c	U_{iso} (Å^2)
C24	− 0.037(2)	0.013(3)	0.174(3)	0.25(1)	C25	0.042(1)	0.045(2)	0.324(2)	0.165(8)
C26	− 0.008(1)	0.044(2)	0.345(2)	0.20(1)	C27	0.208(1)	0.496(3)	1.008(4)	0.26(1)
C28	0.001(1)	− 0.080(2)	0.337(2)	0.19(1)	C29	0.154(2)	0.575(3)	0.542(3)	0.29(2)
C30	0.204(1)	0.447(2)	0.467(2)	0.189(9)	C31	0.012(2)	0.074(3)	0.200(3)	0.28(1)
C32	0.130(1)	0.532(3)	1.001(3)	0.24(1)	C33	0.206(1)	0.521(3)	0.525(3)	0.25(1)
C34	0.133(1)	0.485(3)	0.804(3)	0.27(1)	C35	0.121(1)	0.556(2)	0.876(2)	0.175(9)
C36	0.202(2)	0.423(3)	1.015(4)	0.30(2)	C37	0.178(1)	0.560(2)	0.817(2)	0.22(1)

Bond Length (Å)

C1–N1	1.320(9)	C4–N7	1.293(9)	C7–N13	1.303(9)
C1–N2	1.335(9)	C4–N8	1.304(9)	C7–N14	1.316(8)
C1–S1	1.751(8)	C4–S4	1.733(8)	C7–S7	1.723(8)
C2–N4	1.314(9)	C5–N10	1.310(9)	C8–N15	1.292(9)
C2–N3	1.321(9)	C5–N9	1.316(9)	C8–N16	1.330(9)
C2–S2	1.729(8)	C5–S5	1.715(9)	C8–S8	1.738(8)
C3–N5	1.319(10)	C6–N11	1.314(9)	C9–N18	1.300(8)
C3–N6	1.318(9)	C6–N12	1.348(9)	C9–N17	1.325(9)
C3–S3	1.754(8)	C6–S6	1.735(8)	C9–S9	1.748(8)

Bond Angle (°)

N2–C1–N1	118.6(8)	N8–C4–N7	118.5(8)	N14–C7–N13	119.7(8)
S1–C1–N1	120.5(6)	S4–C4–N7	119.4(6)	S7–C7–N13	117.8(6)
S1–C1–N2	120.2(6)	S4–C4–N8	119.3(6)	S7–C7–N14	122.2(7)
N3–C2–N4	118.2(8)	N9–C5–N10	117.8(8)	N16–C8–N15	115.4(8)
S2–C2–N4	120.3(6)	S5–C5–N10	120.4(6)	S8–C8–N15	124.9(7)
S2–C2–N3	120.1(6)	S5–C5–N9	121.6(7)	S8–C8–N16	119.7(6)
N6–C3–N5	119.1(8)	N12–C6–N11	116.4(8)	N17–C9–N18	119.8(8)
S3–C3–N5	120.6(6)	S6–C6–N11	125.6(6)	S9–C9–N18	119.9(6)
S3–C3–N6	120.3(6)	S6–C6–N12	118.0(5)	S9–C9–N17	120.3(6)

Note. C10 to C37 denote carbon atoms added within the tunnel to represent the contribution to the diffraction pattern from scattering by the guest molecules. The asymmetric unit of the host substructure comprises 9 thiourea molecules in general positions. There are 36 thiourea molecules in the unit cell.

established in the average crystal structure in the low-temperature phase. Nevertheless, there is evidence (see Fig. 6) that the guest molecules exhibit an overall orientational preference, which correlates well with the distortion of the host tunnel. Thus, the plane of the guest molecules (projected onto the plane perpendicular to the tunnel axis) lies along the long "diameter" of the distorted host tunnel, suggesting that the orientation of the guest molecules (with respect to rotation about the tunnel axis) is confined to a comparatively narrow distribution in the low-temperature phase. Nevertheless, while projections of the type shown in Fig. 6 can provide an overall impression of the extent of distortion of the tunnels, we nevertheless emphasize the potential pitfalls that may arise, in general terms, from overinterpretation of two-dimensional structural projections. As found for the high-temperature phase, the guest molecules are positioned preferentially along the tunnel at sites corresponding to the "cages" in the host structure.

5. CONCLUDING REMARKS

Single-crystal X-ray diffraction has been applied to elucidate structural properties of the fluorocyclohexane/thiourea inclusion compound, despite the fact that the crystals are twinned both in the high-temperature and low-temperature phases. At ambient temperature, the host structure is rhombohedral and the guest molecules are disordered. Twinning arises through the coexistence of both obverse and reverse domains of the rhombohedral structure. In the low-temperature phase, the host tunnels are distorted toward lower symmetry from the rhombohedral high-temperature structure. The guest molecules show evidence of an orientational preference in the low-temperature phase, which correlates well with the distortion of the host tunnel. The twinning in the low-temperature phase clearly originates from the obverse/reverse twinning in the high-temperature phase, although the description and handling of the twinning are different as a consequence of the lowering of the symmetry.

It is interesting to contemplate the reasons underlying the fact that crystals of fluorocyclohexane/thiourea exhibit obverse/reverse twinning, whereas crystals of other thiourea inclusion compounds studied previously (such as chlorocyclohexane/thiourea (31)) apparently do not. Detailed investigations of the crystal growth processes and the application of a range of experimental probes to investigate local structural properties are clearly required in order to understand this issue.

The structure determination strategy for twinned inclusion compounds applied in this paper should find wider applications to other solid inclusion compounds, as it is well known that many inclusion compounds exhibit twinning on passing below low-temperature phase transitions (whether or not there is twinning at ambient temperature). The main requirements in solving crystal structures from diffraction data affected by twinning are to identify the type of twinning, to establish the geometric relationships between the different twin components, and to understand the relative contributions of each twin component to each reflection in the measured diffraction data. With significant recent developments in the versatility of structure refinement packages and the concomitant ability of modern diffractometers (particularly area detectors) to record data from twinned crystals in a rational manner, a wide range of twinned structures are now amenable to investigation that could not be studied in the past.

ACKNOWLEDGMENTS

We are grateful to Ciba Specialty Chemicals and the University of Birmingham for the award of a studentship (to L.Y.). We thank Dr. R. Herbst-Irmer and Professor G. M. Sheldrick (University of Göttingen) for valuable discussions on the use of the SHELXL-97 program and Mr. S.-O. Lee (University of Birmingham) for experimental assistance.

REFERENCES

1. B. Angla, *Compt. Rend.* **224,** 402 (1947).
2. B. Angla, *Compt. Rend.* **224,** 1166 (1947).
3. H. U. Lenné, *Acta Crystallogr.* **7,** 1 (1954).
4. K. Takemoto and N. Sonoda, *in* "Inclusion Compounds" (J. L. Atwood, J. E. D. Davies, and D. D. MacNicol, Eds.), Vol. 2, p. 47. Academic Press, New York, 1984.
5. M. D. Hollingsworth and K. D. M. Harris, *in* "Comprehensive Supramolecular Chemistry" (D. D. MacNicol, F. Toda, and R. Bishop, Eds.), Vol. 6, p. 177. Pergamon Press, Oxford, 1996.
6. R. W. Schiessler and D. Flitter, *J. Am. Chem. Soc.* **74,** 1720 (1952).
7. L. C. Fetterly, *in* "Non-Stoichiometric Compounds" (L. Mandelcorn, Ed.), Academic Press, New York, 1964.
8. A. R. George and K. D. M. Harris, *J. Mol. Graphics* **13,** 138 (1995).
9. M. Nishikagawa, *Chem. Pharm. Bull.* **11,** 977 (1963).
10. K. Fukushima, *J. Mol. Struct.* **34,** 67 (1976).
11. A. Allen, V. Fawcett, and D. A. Long, *J. Raman Spectrosc.* **4,** 285 (1976).
12. A. E. Aliev and K. D. M. Harris, *J. Am. Chem. Soc.* **115,** 6369 (1993).
13. M. S. McKinnon and R. E. Wasylishen, *Chem. Phys. Lett.* **130,** 565 (1986).
14. K. Müller, *Magn. Reson. Chem.* **30,** 228 (1992).
15. I. J. Shannon, M. J. Jones, K. D. M. Harris, M. R. H. Siddiqui, and R. W. Joyner, *J. Chem. Soc. Faraday Trans.* **91,** 1497 (1995).
16. A. Nordon, R. K. Harris, L. Yeo, and K. D. M. Harris, *Chem. Commun.* 961 (1997).
17. R. K. Harris, A. Nordon, and K. D. M. Harris, *Magn. Reson. Chem.* **37,** 15 (1999).
18. G. Friedel, "Leçons de Cristallographie," pp. 245–252, 421–493. Berger-Levrault, Paris, 1926. [Reprinted, Blanchard, Paris, 1964]
19. G. Donnay and J. D. H. Donnay, *Can. Mineral.* **12,** 422 (1974).
20. Y. Le Page, J. D. H. Donnay, and G. Donnay, *Acta Crystallogr. Sect. A* **40,** 679 (1984).
21. P. Niggli, "Geometrische Kristallographie des Diskontinuums," p. 551. Borntraeger, Leipzig, 1919.
22. R. Hocart, "Cours du Certificat de Minéralogie et Cristallographie, Atlas," p. 13. Faculté Sci. Centre De Polycopie, Paris, 1958.
23. V. K. Wadhawan, *Acta Crystallogr. Sect. A* **53,** 546 (1997).
24. R. W. Cahn, *Adv. Phys.* **3,** 363 (1954).
25. Molecular Structure Corporation, "TEXSAN, Single Crystal Structure Analysis Software," Version 1.6 (MSC, 3200 Research Forest Drive, The Woodlands, TX 77381, USA), 1993.
26. M. C. Burla, M. Camalli, G. Cascarano, C. Giacovazzo, G. Polidori, R. Spagna, and D. Viterbo, *J. Appl. Crystallogr.* **22,** 389 (1989).
27. G. M. Sheldrick, "SHELXL-97-2, Program for Crystal Structure Determination." University of Göttingen, Germany, 1998.
28. A. J. O. Rennie and K. D. M. Harris, *Proc. R. Soc. A* **430,** 615 (1990).
29. S. van Smaalen, *Crystallogr. Rev.* **4,** 79 (1995).
30. G. M. Sheldrick, "SHELXL-97 Manual," Chap. 6. University of Göttingen, Germany, 1998.
31. K. D. M. Harris and J. M. Thomas, *J. Chem. Soc. Faraday Trans.* **86,** 1095 (1990).
32. M. J. Jones, I. J. Shannon, and K. D. M. Harris, *J. Chem. Soc. Faraday Trans.* **92,** 273 (1996).